Insights on the role of fibres in the laboratory testing of peat

Luis J. Parra-Gómez[1*], *Cristina* Jommi[2,1], and *Stefano* Muraro[1]

[1] Department of Geoscience and Engineering, Delft University of Technology, Delft, The Netherlands
[2] Department of Civil and Environmental Engineering, Politecnico di Milano, Milano, Italy

1 Introduction

Peat is a highly organic soil of considerable geoenvironmental relevance as it plays important roles in carbon storage and hydrology and provides valuable ecosystemic services. In the Netherlands, its widespread occurrence and historic role as a foundation and construction material for embankments, dikes, and transport networks makes describing its mechanical behaviour highly important [1].

Peat is widely recognised for its extreme compressibility, often experiencing volume changes greater than 50% during compression [2–3]. Paradoxically, this high compliance coexists with high shearing resistance. Experimental evidence from triaxial and simple shear tests indicates that peat can sustain very high shear stress ratios, with reported friction angles frequently exceeding 35° and in some cases approaching the tension cut-off condition (i.e. 90°) [3–6]. Peat undergoes substantial internal rearrangement and large deformations while mobilising its strength.

This distinctive mechanical response is generally attributed to its fibrous fabric. Unlike mineral soils, peat solids form an interconnected network of organic fibres with varying sizes, orientations, and degrees of decomposition [7–8]. Multi-scale aggregations sustain an extremely porous and highly deformable skeleton, while simultaneously providing mechanical reinforcement through the tensile engagement of larger fibres. This reinforcing effect introduces important challenges in the interpretation of conventional laboratory tests, and systematic differences in shear strength parameters are commonly observed between triaxial tests, direct simple shear tests, and field back-calculations [4–6]. Differences are generally attributed to the fibre reinforcement being dependent on the orientation of the fibres relative to the loading direction and the boundary conditions imposed during testing.

Recently, Parra-Gómez et al. [9] proposed a numerical framework to model the constitutive behaviour of peat, accounting for the fibre reinforcement and explicitly considering the fabric rearrangement that the material experiences upon loading. This numerical framework is exploited here to derive insights into the role of fibre reinforcement in the interpretation of conventional laboratory tests.

2 Modelling framework

The framework conceptualises peat as a composite of a continuous matrix and a discrete fibre network (Figure 1a). The matrix is described by a three-dimensional continuum with a constitutive behaviour that, in principle, could follow any conventional constitutive response of porous media. In this work, the model proposed by Muraro & Jommi for reconstituted peat is adopted, as it captures distinct features of the yield locus, plastic potential and hardening law of the material [6]. The fibre network, instead, is described as an assembly of purely axial elastic and perfectly plastic one-dimensional elements which act as kinematic constraints. In tension the fibres yield with ductility and eventually break, while they buckle in compression. The collective contribution of the individual fibres to the macroscopic response is computed through homogenisation of their forces following the Gauss-Ostrogradsky theorem. The stress tensor of the overall composite $\boldsymbol{\sigma}$ is computed from the addition of the stress tensor of the matrix $\boldsymbol{\sigma}_m$ and the homogenized tensor of the fibre assembly $\boldsymbol{\sigma}_f$. Strains are assumed to be the same in all constituents, such that:

$$\boldsymbol{\sigma} = \boldsymbol{\sigma}_m + \boldsymbol{\sigma}_f \quad ; \quad \boldsymbol{\varepsilon} = \boldsymbol{\varepsilon}_m = \boldsymbol{\varepsilon}_f = \frac{1}{2}\log(\mathbf{F}^{\mathrm{T}}\mathbf{F}) \tag{1}$$

The framework adopts finite strain kinematics to account for fibre reorientation and changes in volumetric proportions during deformation. The natural strains of the composite, $\boldsymbol{\varepsilon}$, and its constituents, $\boldsymbol{\varepsilon}_m$ and $\boldsymbol{\varepsilon}_f$, are computed from the deformation gradient tensor, $\mathbf{F}$, of the motion $\boldsymbol{\chi}$. Under the assumption of homogenous and linear motion, $\mathbf{F}$ defines a linear map between the initial material position of the fibres and their current deformed configuration.

Fibre geometry, orientation, and mechanical properties are modelled stochastically using experimentally measured distributions. Fibres are taken as cylindrical elements with random diameters following a log-normal distribution and a constant aspect ratio. The initial orientations of the fibres follow a fibre orientation distribution (FOD), $\rho(\theta,\phi)$, which defines the probability of a fibre being oriented along a longitude, θ and latitude, ϕ such that:

$$\int_{-\pi}^{\pi}\int_{-\pi/4}^{\pi/4} \rho(\theta,\phi)\cos\phi \, \mathrm{d}\phi \, \mathrm{d}\theta = 1 \tag{2}$$

* Corresponding author: L.J.ParraGomez@tudelft.nl

The FOD $\rho(\theta,\phi)$ can take any functional form that satisfies Eq. (2), and its invariant under reflection through the origin; in this work a three-dimensional supershape function is adopted (Figure 1a). Tensile strength and stiffness of the fibres are modelled as random variables with a modified Weibull distribution. Notably, both strength and stiffness are inversely correlated with fibre size, and this is implemented through the adoption of a weak link scaling law. Additional details on the formulation and the experimental data used to derive parameters can be found in [9].

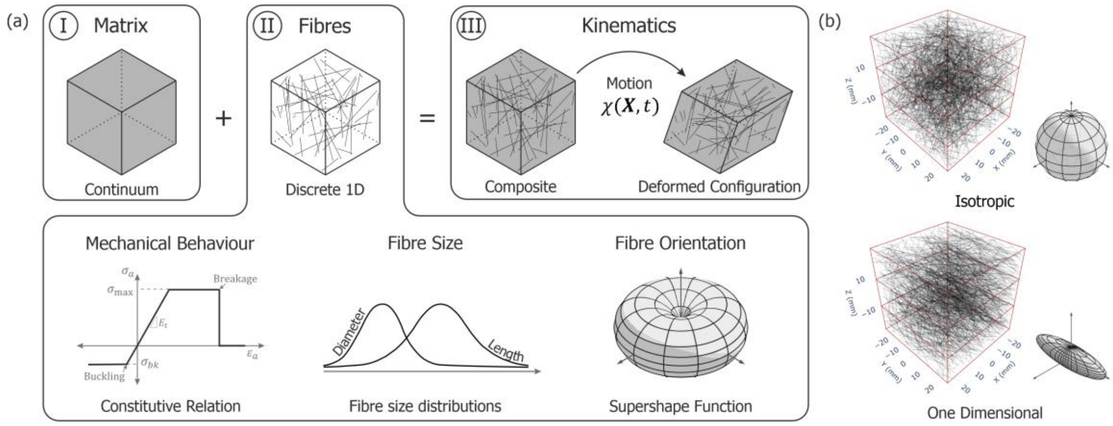

Figure 1. (a) Conceptual framework for the modelling of peat as a composite; (b) examples of fibre arrangements with different FOD.

3 Numerical simulations

Cubic samples of peat with a size of 50 mm were used to explore the implications of fibre reinforcement along common stress paths used in laboratory testing. An assembly of fibres was simulated with a spatially uniform distribution within the volume, adjusting the number of fibres to match a volumetric fibre content of 20%, and selecting fibre orientations in accordance with a prescribed FOD distribution. Figure 1b shows two examples of sample realisations. The process to generate the numerical samples and the properties of the fibre and matrix are reported in detail in [9]. Simulations were then conducted in a controlled strain approach by applying linear deformation gradient increments to the samples.

3.1 Loading direction and fibre reorientation

The importance of the kinematics adopted for fibre reinforcement was evaluated by comparison of a sample simulated within the proposed framework with an identical one analysed under infinitesimal strain assumptions. The initial FOD of the sample was modelled to match the data reported by Kettridge & Binley [8], which shows a preferential horizontal fibre orientation. The sample was first subjected to isotropic compression to a volumetric strain of 0.4 and then sheared isochorically up to a deviatoric strain of 0.4 along four shearing paths representative of undrained laboratory tests: triaxial compression (TXC), triaxial extension (TXE), simple shear (SS), and plain strain compression (PS). Figure 2a illustrates the deformation modes associated with each loading path and their directions in the strain π-plane.

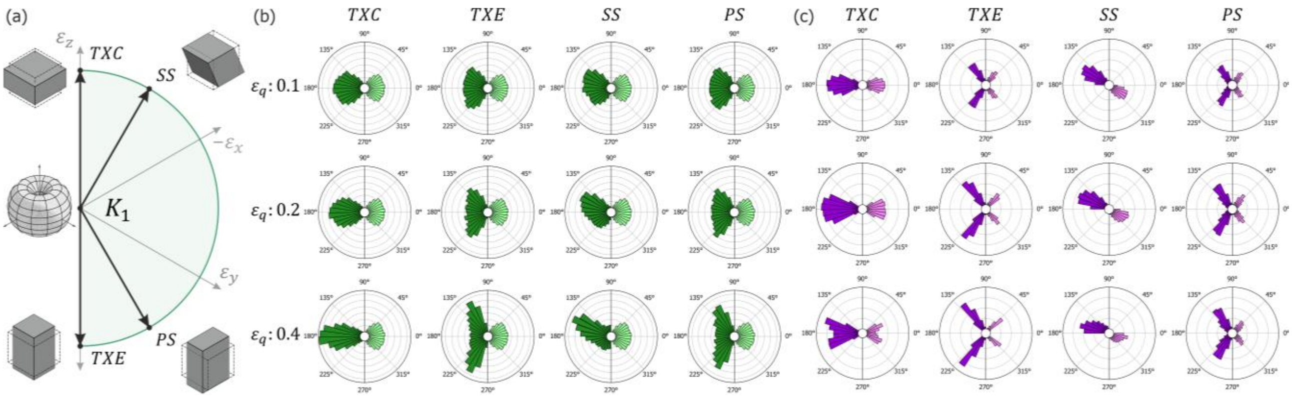

Figure 2. Micromechanical evolution of fibres over four isochoric shearing paths. (a) strain paths in the π-plane; (b) latitude polar plots of the FOD for different deviatoric strains; (c) polar plots for fibre reinforcement at different deviatoric strains. Dark tones denote finite strain kinematics in the left and light tones show infinitesimal kinematics on the right.

Figure 2b shows polar plots of the orientation density as a function of the latitude angle, ϕ. To facilitate the comparison, half of each distribution is shown on either side of the same diagram: finite strain on the left and infinitesimal strain on the right. The figure shows the evolution of the fibre orientation distribution at different shearing strains. In the infinitesimal case, the distribution remains fixed, whereas under finite strain kinematics the shape of the distribution changes dramatically throughout loading. The distribution progressively aligns with the direction of minor principal strain. For TXC the fibres align towards the horizontal direction, whereas for TXE and PS they align towards the vertical one. The rotation is most evident for SS, where the fibres progressively align towards an orientation of 135°.

Figure 2c shows the directional fibre reinforcement defined as the product of axial stress and fibre density. The influence of kinematics is most evident here, with the infinitesimal formulation consistently producing lower reinforcement for all loading paths and orientations. Rotation of the fibres towards the minor principal strain direction, allows the material to engage a larger number of fibres in tension and maximises their deviatoric reinforcement. Notably, consideration of finite strains implies that all possible shearing paths will cause reorientation of the fabric and inexorably lead to tensile engagement of the fibres irrespective of the initial FOD of the material.

Figure 3 compares the kinematic assumptions in terms of the invariants of the composite stress tensor, $\boldsymbol{\sigma}$. Finite kinematics produce differences of approximately 10 to 20% in volumetric and von Mises stresses at deviatoric strains above 0.1. Notably the volumetric stress diminishes, and the Mises stress increases, which together lead to a significant increase in the mobilised stress ratio. Consequently, the interpretation of the friction mobilised by the material is highly sensitive to the kinematic description and the loading direction.

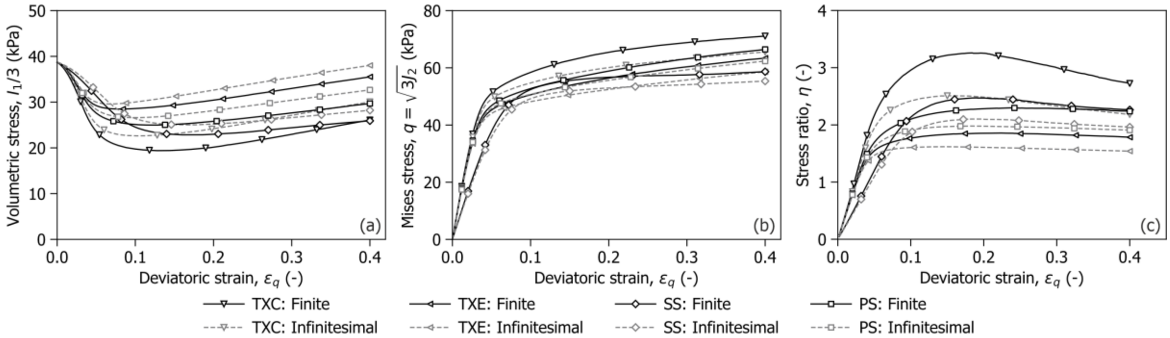

Figure 3. Evolution of the composite stress tensor invariants with deviatoric strain. (a) volumetric stress; (b) von Mises stress; (c) stress ratio.

3.2 Initial fibre anisotropy

Fibre reinforcement also depends on the initial orientation distribution and its alignment with the loading direction. This is explored in Figure 4, where the shearing paths from Figure 2a were imposed on samples with different initial FOD. Besides an isotropic reference, three distributions where fibres are preferentially aligned towards the horizontal were modelled: one one-dimensionally aligned with the y axis and two vertically restricted (KB1 and KB2) with increasing levels of anisotropy. Figure 4 shows the influence of the initial fibre orientation distribution on the overall response of the composite.

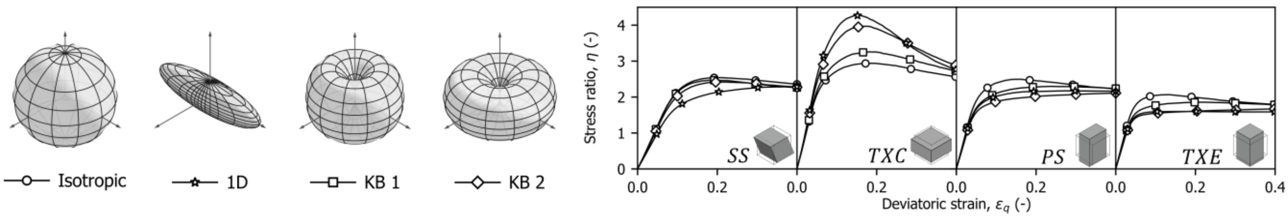

Figure 4. Influence of the initial fibre orientation on the fibre response for four isochoric shearing paths.

Overall, changes in the orientation distribution produce relatively small variations in the absolute magnitude of the von Mises and volumetric stresses (5% to 20%). However, again, both effects compound to more significant differences in the stress ratio of the material. The TXC shearing path shows the greatest variation across the examined distributions. This is likely due to the preferential alignment of the FODs, which coincides with the minimum strain direction TXC. Smaller variations are observed in SS.

Given the geological process that led to peat formation, peat fibres are expected to be preferentially aligned in the horizontal direction [3,8]. Since the TXC path is the most common loading condition in conventional triaxial tests, a strong sensitivity of the composite response to the initial fibre orientation distribution may contribute to explain the wide dispersion of results reported for peat samples in triaxial testing and the preference for simple shear of the practice. However, this disadvantage of triaxial testing is tangible only if the analysis of the material response is limited to a single loading direction. If multiple directions are analysed, variations of the mechanical response can be exploited to indirectly characterise the fibre orientation distribution, which to date remains unfeasible to experimentally derive in most practical applications.

Figure 5 illustrates the analysis of a pair of peat samples subjected to two loading conditions. Conventional triaxial tests were performed on undisturbed peat samples taken in proximity to the same block sample. Both samples were saturated under a back pressure of 300 kPa and isotropically compressed at a rate of 8 kPa/day to a mean effective stress of 50 kPa (A to B). After compression, drainage was closed and the samples were sheared at constant volume along strain-controlled triaxial compression (TXC) and extension (TXE) at a rate of 0.015 mm/min (B to C). The tests were modelled with the proposed framework using three different initial FOD, inspired by the data of [8] and modified to have increasing levels of anisotropy (D1, D2, and D3). For reference, predictions for the composite are plotted together with the response of a sample without any fibre reinforcement.

The simulations reproduce two key features of peat behaviour: the mobilisation of very high stress ratios, reaching the Tension Cut-off Line (continuous red line shown in Figure 5b and Figure 5c), and the characteristic change in the stress path curvature above the critical state stress ratio [4–7].

During shearing, the overall evolution of the sample stress path closely follows the experimental measurements up to the critical state stress ratio (CSL) of the matrix (dotted grey line in Figure 5b and 5c). Differences between the three distributions become apparent beyond this point, with the D2 distribution providing the best match to the experimental data in both compression and extension paths. The response is highly sensitive to the anisotropy, as more horizontal fibres lead to higher reinforcement in compression but lower engagement in extension and vice versa. This consistent change makes it possible to use the pair of triaxial stress paths to indirectly assess the shape of the FOD distribution.

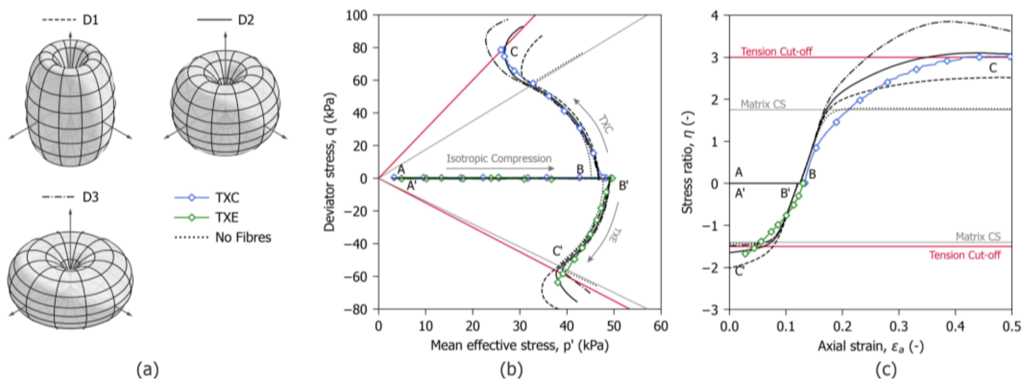

Figure 5. Comparison between triaxial tests on peat samples and the proposed numerical formulation. (a) variations of initial FOD for the sample; (b) stress paths; (c) evolution of the stress ratio of the samples with deviatoric strain.

4 Conclusions

The results highlight the fundamental role of fibre kinematics in governing the mechanical response of peat. Fibre reorientation induced by large strains significantly alters the mobilisation of reinforcement, leading to measurable differences in stress invariants and stress ratios. Notably, fibres cannot be disregarded in any loading direction, as deformation inevitably leads to their rotation towards the direction of minimum principal strain, promoting tensile engagement. As a result, the assessment of mobilised friction is highly sensitive to the kinematic description and the imposed loading path.

The interaction between fibre orientation and loading direction provides a possible explanation for the variability observed in laboratory testing. In particular, a TXC, where the minimum principal strain aligns with the horizontal fibre orientation, maximises the sensitivity of the response to the initial fabric and may contribute to the dispersion of experimental results. The results suggest that testing under multiple loading directions offers a practical route to indirectly characterise fibre orientation and reinforcement. A testing strategy for peat should embrace fibre reinforcement as an inherent and inextricable part of peat response and adopt testing protocols that exploit fibre reorientation for material characterisation.

References

1. G. Kruse, E. den Haan (2006). Characterisation and engineering properties of Dutch peats. In: Characterisation and Engineering Properties of Natural Soils.
2. H. Yamaguchi, Y. Ohira, K. Kogure (1985). Volume change characteristics of undisturbed fibrous peat. Soils Found., **25**(2), 119–134.
3. G. Mesri, M. Ajlouni (2007). Engineering properties of fibrous peats. J. Geotech. Geoenviron. Eng., **133**(7), 850–866.
4. M.T. Hendry, J.S. Sharma, C.D. Martin, and S.L. Barbour (2012) Effect of fibre content and structure on peat strength. Can. Geotech. J., **49**(4), 403–415.
5. B.C. O'Kelly (2017). Measurement, interpretation and recommended use of laboratory strength properties of fibrous peat. Geotech. Res., **4**, 136–171.
6. S. Muraro, C. Jommi Pre-failure behaviour of reconstituted peats in triaxial compression. Acta Geotech. 2021;**16**(3):789–805.
7. A.O. Landva, P.E. Pheeney (1980). Peat fabric and structure. Can. Geotech. J., **17**(3), 416–435.
8. N. Kettridge, A. Binley (2008). X-ray computed tomography of peat soils: measuring gas content and peat structure. Hydrol. Process., **22**(25), 4827–4837.
9. L.J. Parra-Gómez, C. Jommi, S. Muraro (2025). The role of finite strain kinematics in the natural fibre reinforcement of peat and other soft organic soils. Sci. Rep., **15**, 41875.